Journal of Engineering and Applied Sciences 12 (24): 7539-7547, 2017
ISSN: 1816-949X

Behavior Study of Top Seat Angle Steel Beam to Column Connections

Kamal Ahmed Al-Fakih, Siew Choo Chin and Shu IngDoh
Faculty of Civil Engineering and Earth Resources, Universiti Malaysia Pahang,
26300 Gambang, Pahang, Malaysia

Abstract: The aim of this present study was simulating the behavior of Top Seat Angle (TSA) steel connections by using Finite Element Analysis (FEA) computer software, known as "ABAQUS". The purpose of this study is to provide the basis for the fastest and most economical design and analysis and to ensure the required steel connection strength. For this study, started used review method of behavior of steel beam-to-column bolted connections. Two models of different cross-section were examined under the effect of concentrated load and different boundary conditions. In all the studied case, material nonlinearity was accounted. A sample study on TSA connections was carried out using both material and geometric nonlinearities. This object will be of great value to anyone who wants to better understand the behavior of the steel beam to column connection. The results of the study have a field of reference for future research for members of the development of the steel connection approach with simulation model design.

Key words: Top-seat angle connections, simulation, moment-rotation, ABAQUS, FEM (Finite Element Method), Malaysia

INTRODUCTION

Many manufacturers, erectors and fabricators prefer to use a simple fabricated connection that can be easily assembled and installed such as joints that use bolts in assembly rather than weld joints. Welding joints require more time coupled with high-skilled labor. Therefore, many steel manufacturers preferred bolted connections in the field. Steel connections are classified into two types: The first type is Partially Restrained (PR) and the second is Fully Restrained (FR). It is assumed in the design of steel connections that the FR-connections have enough stiffness to maintain the angles between the members of the crusade. It is also assumed that the PR-connections have the insufficient stiffness to maintain the angles between the members of the crusade. When it is not considered to restrict the connection, usually called the framing is simple. These joint connections are the overload that results from other factors like welding fasteners, loads side and gravity.

The experimental results will be used to find usable limit states and to improve a rational design procedure for bolted connections similar to the connections under consideration. The proposed study focalizes on understanding the behavior of steel connections subjected to shear or moment loads using finite element method. The aim of this study is to provide moment-rotation characteristics and corresponding parameters of semi-rigid beam-to column connections theoretically using the ABAQUS computer program. Affect the flexibility of the connections of both the power distribution and the deformation in columns and beams of the frame and the frame must be calculated in the structural analysis. It is assumed that the flexible analysis of linear distortions is relatively small and equilibrium equations can be formulated with respect to the initial engineering. Several types of research were conducted concerning the behavior and design of steel connections. The aim was to establish a better understanding and improved techniques for evaluation of the connections between beams and columns under the effect of shear and moment loads. Ahmed and Hasan (2015) presented a research study for the nonlinear analysis of the Finite Element (FE) of the angle connections as known top-seat angle connections. This analysis was done using the ABAQUS program to investigate the effect of conductivity parameters and properties on the evolving motion by performing the simulation tests on 16 samples from the previous references. Compared with the results of the analysis of finite elements with experimental results to study the applicability of the model, the results were close to each other. Pirmoz *et al.* (2009) investigated the behavior of bolted TSA connections whereby a new moment-rotation relation is provided. Many developed models have refined 3D finite element based on previous experimental studies and the accuracy of result

Correspondig Author: Kamal Ahmed Al-Fakih, Faculty of Civil Engineering and Earth Resources, Universiti Malaysia Pahang, 26300 Gambang, Pahang, Malaysia

is verified by comparing experimental results with that of the published numerical models and old studies. It is evident that this type of model has the ability to analyze and evaluate the behavior connection of moment-rotation under the combined axial tension load and moment load which largely corresponds to what it is in the reality. Xinwu (2007) studied the behavior of semi-rigid connections under cyclic reversal loading. Three full-scale specimens of steel angles using H-section members had been conducted. The aim of this is to know the behavior of these types of connections under loading in a range of plastics and make sure that the effect of the parameter design suchas pre-tension of bolts, column flange stiffener and thickness of flange angle on the general behavior of connections. The experimental results showed a decrease in hardness with load cycles due to contraction of the pre-tensioning bolt forces and the deterioration of connection properties and inflexible distortions. The main reason is that the stiffness of TSA was too weak. Liew *et al.* (1993a, b), part 1 and 2 was developed and generalized the connection parameters for framing angle connections, TSA, DWA and TSA-DWA connections. The analysis of second order frames was used to calculate the moments in these designs. The perfect result in any partially restricted frame is to achieve balance in the final and mid-range moments. The interest part in this connection is that it can simply be detailed to limit the resistance by the amount of top reinforcement with the availability of DWA suitable stiffness.

The behavior of a connection is described by its moment-rotation curve. Figure 1 shows the relative rotation-Ø of a typical connection due to Moment-M, acting on the beam of the connection (Kishi and Komuro, 2011).

Moment-rotation curves for some connections usually use PRCs as shown in Fig. 2. It can be seen that TSA and TSA-DWA connections are amongst the stiffest connection.

There are many researchers who have studied the behavior of the column connection to beam and simulate it using computer software (Danesh *et al.*, 2007; Hean *et al.*, 2016; Daryan and Yahyai, 2009; Stelmack *et al.*, 1986; Kukreti and Abolmaali, 1999; Dai *et al.*, 2010).

MATERIALS AND METHODS

Modeling and simulation

Experimental specimen description: The experimental data usedin the proposed study had been obtained from the studies reported by Stelmack *et al.* (1986) for top seat angle connections. The detail of a TSA-connection is as

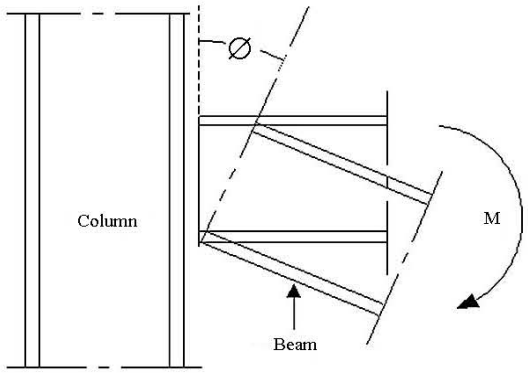

Fig. 1: Connection moment-rotation behaviors

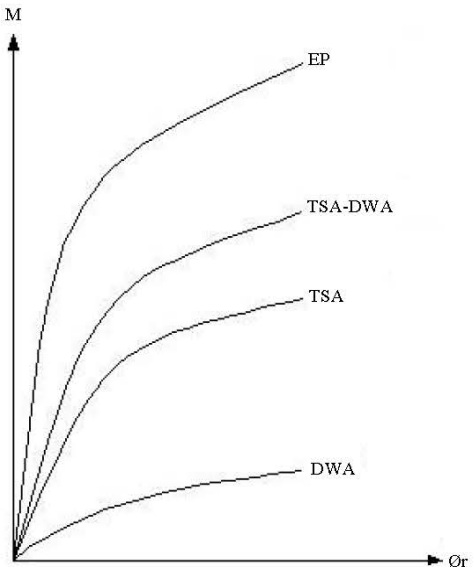

Fig. 2: Typical moment rotation curve of beam-to-column connections

shown in Fig. 3. To prove the connection model predictions, comparisons were made with the full-scale test results of connections that have material and component compatibility (connection components made from A36 steel and 19.1 mm A325 bolts). In the present analysis, the flexible frame study conducted by Stelmack *et al.* (1986) was considered. A summary of TSA-connections geometries is as indicated in Table 1 and 2.

Finite element modeling: ABAQUS program can organize and analyze complex structural problems and shapes inclusive of three-dimensional structures. In this type of software, technology lies in finding the proper way the development of mesh-arrangement. It should balance the

Table 1: Connection geometry of (Stelmack *et al*., 1986) for (TSA-connections)

Test ref.	Beam size (mm×kg/m)	Column size (mm×kg/m)	Gage (mm)	Flanges-angle size (mm)	Fastener (mm)
D1.1/4-1	W130×23.8	W130×23.8	63.5	102×102×6.4×127	A325-19.1
B.1/2-1	W130×23.8	W130×23.8	63.5	102×102×12.8×127	A325-19.1

Table 2: Columns and beams geometric dimensions and yield stresses of (Stelmack *et al*., 1986)

Test ref.	d (mm)	b_f (mm)	t_w (mm)	t_f (mm)	A (mm)	L (Column) (mm)	L (Column) (mm)
D1.1/4-1	127.3	127	6.10	9.10	3020	500	850
B.1/2-1	127.3	127	6.10	9.10	3020	500	850

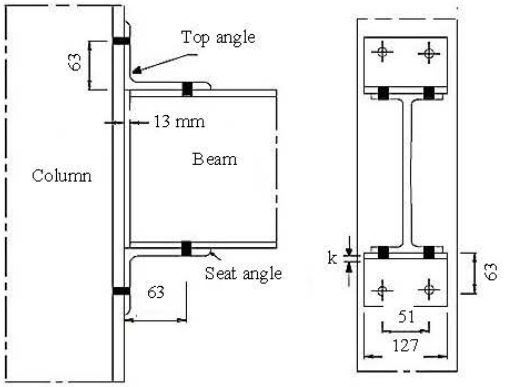

Fig. 3: Typical end-plate connections (Stelmack *et al*., 1986)

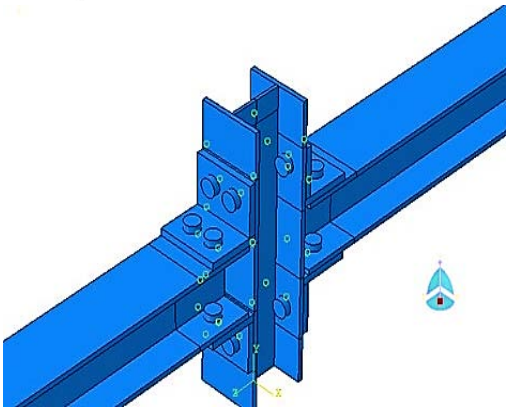

Fig. 4: End-plate connections

size of the mesh-an arrangement between the need for a fine mesh to give an accurate distribution of stress and time reasonable analysis. The perfect solution is the use of fine mesh in areas with high pressures and a coarser mesh in the remaining areas. For all types of connection models, the connection was arranged symmetrically around a vertical medial line as shown in Fig. 4. The members properties and diminutions are used in those models shown in Table 1 and 2 inclusive.

Types of elements: The type of element for beam, column and bolt are 3-Dimensional (3D) Solid brick-element

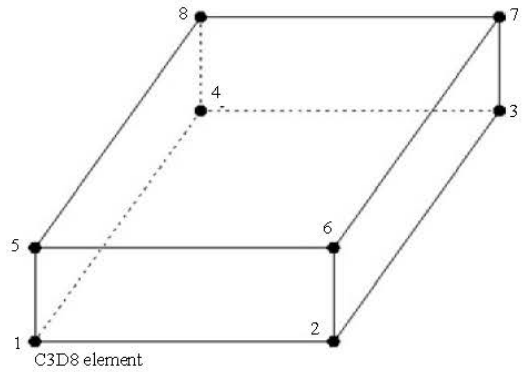

Fig. 5: ABACUS element types

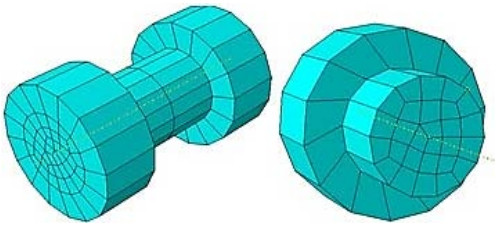

Fig. 6: Bolt mesh arrangement

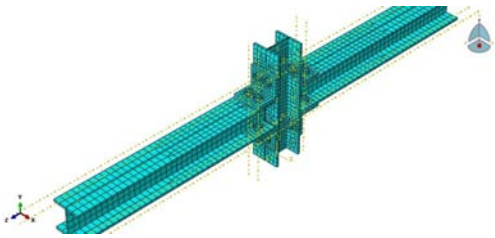

Fig. 7: Complete beam models with final arrangement

finite element model used are available in ABAQUS as shown in Fig. 5. It comprises of eight nodes, each node having three degrees-of-freedom. This element has the capability to model plasticity, large deflection, large strain behavior and uses reduced integration method. The final arrangement of mesh discretization for bolt model shown in Fig. 6. The complete beam model with a final arrangement of mesh discretization is shown in Fig. 7.

Non-linear materials behavior: The material non-linearity definitions took an important role in finite element

Table 3: Material non-linearity properties

Type of element	Yield stress (MPa)	Ultimate stress (MPa)	Modulus of elasticity gap	Poisson ratio
Beam, column and plate	248	483	207	0.3
Bolts	634	828	210	0.3

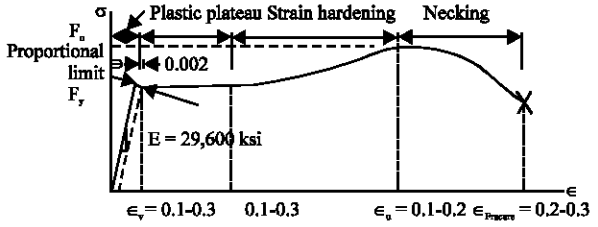

Fig. 8: A typical stress-strain diagram for mild-carbon steel (Stelmack *et al*., 1986)

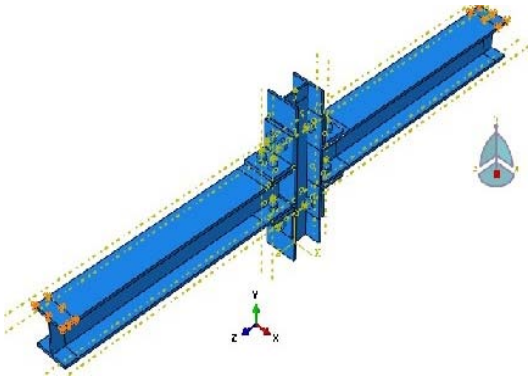

Fig. 9: Boundry conditions and loads

analysis where each definition for different parts of a connection should be carefully thought out. That is, the main connection elements such as beams, columns, flanges, web-angles, bolts and nuts, must be all simulated using the appropriate material parameters and models. Material non-linearity occurs when the stress-strain relationship ceases to be linear, whereby the steel yields and becomes plastic. As a matter of fact, the mild carbon steel ASTM A36 used in the analyses of both Azizinamini and Radziminski (1989) can have different strain-stress diagrams by applying different loading rates and temperature. Otherwise, loading rate is a defined property by the experimental research considered for analysis in this research where the rate of the loading of the investigated connections is related to the monotonic loading case and steel takes the lower yield point and almost follow the exact path of the stress-strain diagram found in any steel design handbook. The figure that explains the regions of such stress-strain diagram is provided in Fig. 8 for convenience. The three sets of material data were as follows.

All elements were defined as elastic isotropic properties for all elastic data. Experimental materials were obtained from all steel tests and the curves allow strain/stress on the basis of actual values instead of theoretical values. The completion of tensile tests on a set of screws allows the properties of the material to be as accurate as possible. Von-Misses yield criteria were used for all types of steel connections. For the plastic, elastic dataset bolts and other members were defined as illustrated in Table 3.

Boundary conditions: The boundary conditions that have been applied to this type of connections prevented displacement in the X, Y, Z directions. Figure 9 restricts the support for the end of the packet (curve U1 = U2 = U3 = 0) as shown in Fig. 9.

Loads: The loading was via. concentrated load acting at a point on the center model. The load is added to the load control file in the window of loads to reach the desired scale of the connections bending moments. The load factor step was specified as 1 and the maximum load factor is also set to 100 with the maximum load factor change in each iteration automatically. The load applied for specimen D1.1/4-1 is 12 and 48 KN for specimen B.1/2-1 (Kukreti and Abolmaali, 1999).

RESULTS AND DISCUSSION

Results of Analysis: In all cases, the inputs and outputs are based on the description in this section for load factor 1-100 set. The maximum load factor of change in each iteration automatically.

Specimen D.1/2-1: The deformation plot as shown in Fig. 10 and 11 are performed using a scale factor of 1.0 to make the displacement clearly visible.

The thick shell element stresses and solid element cannot be in in a single frame because they have different degrees of freedom. Node 626 from the beam was selected for finding the displacement analysis at this node. In addition, the node 626 selected was located at the top of the beam end at 0.850 m from the end support as shown in Fig. 12. The connection rotates at Ø as shown in Fig. 12. The connection rotation is defined as:

$$\varnothing = \tan^{-1}\left[\frac{\Delta x}{h}\right] \Delta x = \left[D_{xt} - D_{xb}\right] \quad (1)$$

Where:

Ø = Relative rotation of connection
D_{xt} = Top horizontal displacement of node 626
D_{xb} = He bottom horizontal displacement of node 556
h = Beam depth (0.127 m)

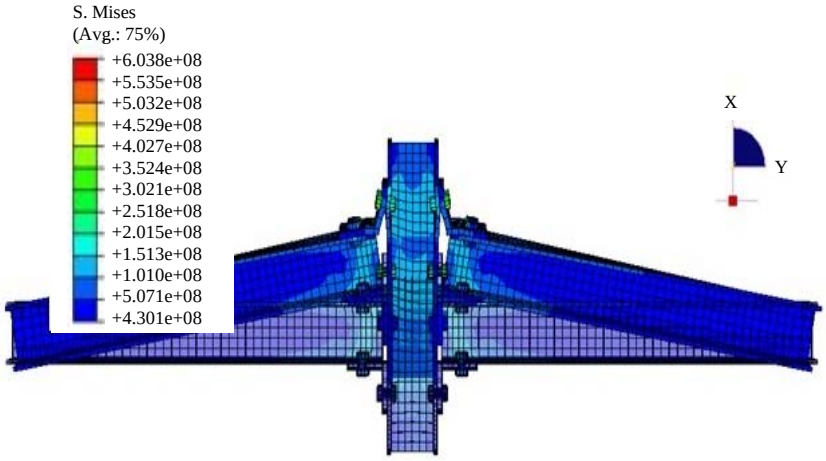

Fig. 10: Deformation of connection plot of spaeciman D.1/2-1

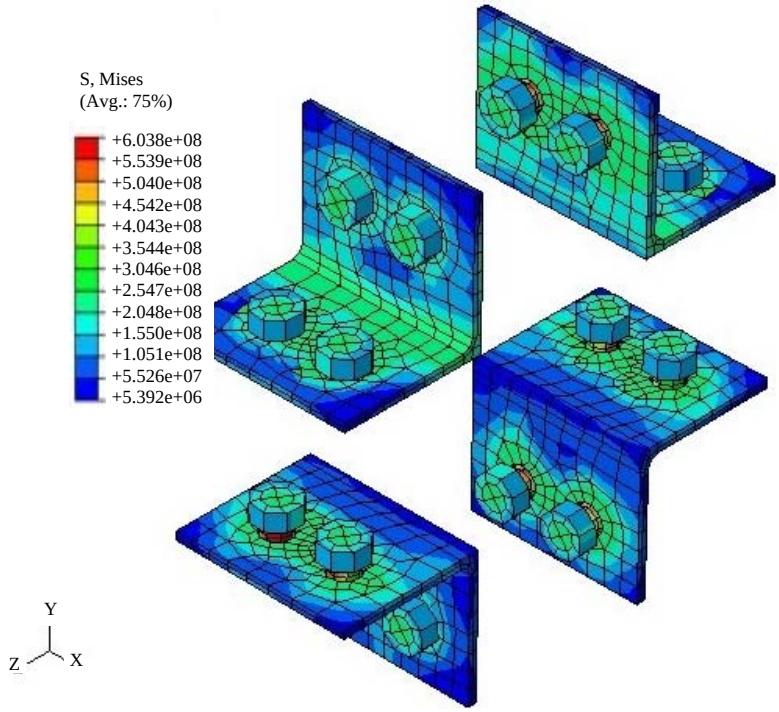

Fig. 11: Connection deformation plot for seat and top angles of specimen D.1/2-1

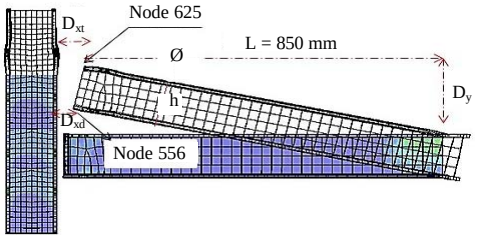

Fig. 12: Connection deformed shape showing nodes 626 and node 556 of specimen D.1/2-1

The rotation Ø in radian unit while linear measurements are in meter's unit. The applied moment was calculated using the following equation:

$$M = \text{Load factor} \times 0.5 \times L$$

Where (M) is applied moment in kN.m acting 0.850 m from the support, (L) is the length of the beam. Numerical results for the calculated loads and displacements are shown in Table 4.

Table 4: Load versus and Displacement (D_y) for specimen D.1/2-1

Load-step	Displacement-D_y (m)	Load (kN)
1	0.00000000	0.00
2	0.00000071	0.05
3	0.00000180	0.08
4	0.00000341	0.12
5	0.00000700	0.17
6	0.00001478	0.25
7	0.00003157	0.37
8	0.00006710	0.55
9	0.00045279	0.81
10	0.00073945	1.21
11	0.00110550	1.81
12	0.00163205	2.71
13	0.00240294	4.07
14	0.00414273	6.09
15	0.00894125	9.13
16	0.01064740	9.85
17	0.01460270	10.93
18	0.02018640	12.00

Table 5: Callculated moments and corresponding rotations for specimen D.1/2-1

Load step	D_{xt} (m)	D_{xb} (m)	Δ_x/h	M (kN.m)	Ø (rad)
1	0.00000000	0.00000000	0.00000000	0.00	0.00000000
2	0.00000047	0.00000037	0.00000076	0.02	0.00000076
5	0.00000120	0.00000096	0.00000196	0.03	0.00000196
4	0.00000228	0.00000180	0.00000376	0.05	0.00000376
5	0.00000457	0.00000358	0.00000775	0.07	0.00000775
6	0.00000917	0.00000708	0.00001640	0.11	0.00001640
7	0.00001768	0.00001323	0.00003504	0.16	0.00003504
8	0.00003221	0.00002276	0.00007445	0.23	0.00007445
9	0.00012011	0.00005731	0.00049450	0.35	0.00049450
10	0.00019418	0.00009203	0.00080438	0.52	0.00080438
11	0.00028992	0.00013771	0.00119850	0.77	0.00119850
12	0.00042729	0.00020335	0.00176326	1.15	0.00176326
13	0.00062715	0.00029859	0.00258713	1.73	0.00258713
14	0.00107821	0.00051546	0.00443109	2.59	0.00443106
15	0.00234413	0.00113682	0.00950638	3.88	0.00950609
16	0.00280212	0.00136445	0.01132024	4.19	0.01131975
17	0.00387544	0.00189672	0.01558047	4.64	0.01557921
18	0.00541266	0.00266452	0.02163890	5.10	0.02163552

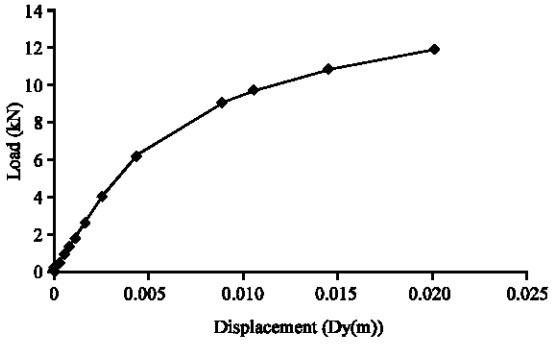

Fig. 13: Load-versus vertical displacement (D_y) at node 626 of specimen D.1/2-1

The total vertical displacement against the total load factor graph for node 626 as shown in Fig. 13. Full computer results and the calculated moment and rotations Ø are shown in Table 5. The moment-rotation (M-Ø) curvefor specimen D.1/2-1is shown in Fig. 14. These diagrams are used to calculate the rotation of the beam and the column.

Table 6: Load versus and Displacement (D_y) for specimen B.1/2-1

Load-step	Displacement-D_y(m)	Load (kN)
1	0.000000	0.00
2	0.000096	0.19
5	0.000164	0.38
4	0.000239	0.66
5	0.000326	1.08
6	0.000436	1.71
7	0.000580	2.66
8	0.000778	4.08
9	0.001060	6.22
10	0.001475	9.42
11	0.002082	14.23
12	0.003018	21.44
13	0.005566	32.25
14	0.007542	36.19
15	0.018210	42.09
16	0.024212	48.00

Specimen B.1/2-1: The deformation plot as shown in Fig. 15 and 16 are performed using a scale factor of 1.0 to make the displacement clearly visible. Numerical results for the calculated loads and displacements are shown in Table 6.

The total vertical displacement against the total load factor graph for specimen B.1/2-1 as shown in Fig. 17. These diagrams are used to calculate the rotation of the beam and the column. The result and the calculated rotations Ø and moments from the computer analysis are shown in Table 7.

The experimental data is obtained from Stelmack *et al.* (1986), Kukreti and Abolmaali (1999). The M-Ø chart for both the large-scale experimental test results and ABAQUS analysis results are plotted and the yield moments of the connection are determined by the intersection of the two tangents as shown in Fig. 18.

Discussion of results: Based on the charts shown in Fig. 14 and 18 and analysis results; summary of the results for both specimens of TSA connections are shown in Table 8.

From Fig. 14, 18 and Table 8, it was found that the determination of yield moment of the connection according to computer analysis software; ABAQUS is against the experiment with a difference of 5.26% for the specimen D.1/2-1 while in the specimen, B.1/2-1 was 2.8%. In addition, from the ABAQUS Software analysis, the yield moment was higher than the experimental test and the ultimate moment is h igher than the experimental test for the specimen D.1/2-1. Whereas in the specimen B.1/2-1, the yield moment was lower than the experimental

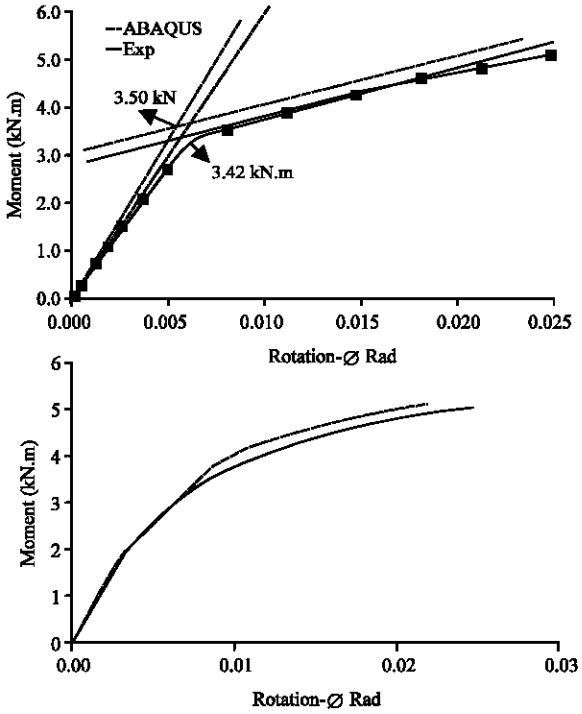

Fig. 14: Moment-rotation (M-Ø) curvefor specimen D.1/2-1

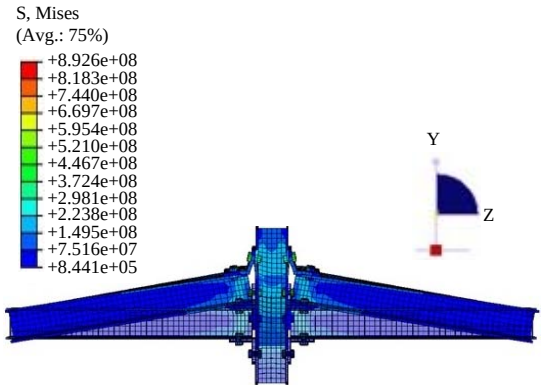

Fig. 15: Deformation of connection plot of specimen B.1/2-1

test and the ultimate moment is higher than the experimental. Furthermore, the ultimate moment values from computer analysis were very close from the experiment for both specimens. Furthermore, the displacement of computer analysis is less than the experience by a very simple difference. Finally, it can also be noted that the computer model seems to be less stiff than the experimental model at lower loads up to the yield moments, after which the experimental model showed stiffer behavior than the ABAQUS numerical results.

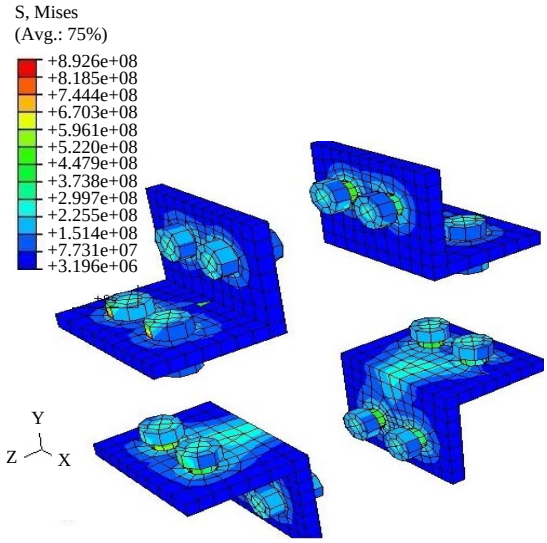

Fig. 16: Connection deformation plot for seat and top angles of specimen B.1/2-1

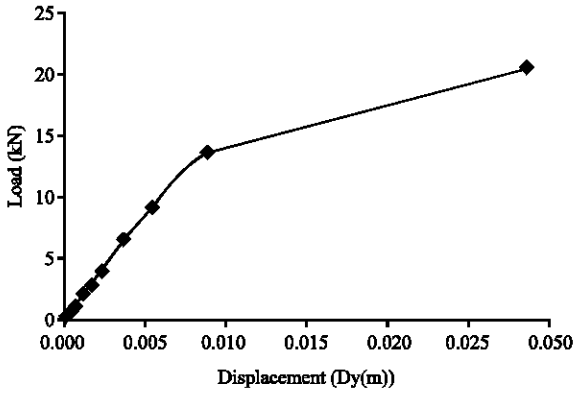

Fig. 17: Load-versus vertical displacement D_y for specimen B.1/2-1

Table 7: Calculated moments and corresponding rotations for specimen B.1/2-1

Load step	D_{x1} (m)	D_{x2} (m)	Δ_x/h	M (kN.m)	Ø (rad)
1	0.000000000	0.000000000	0.000000000	0.00	0.000000000
2	0.000001534	0.000012080	0.000107196	0.08	0.000107196
5	0.000002917	0.000020067	0.000180982	0.16	0.000180982
4	0.000004774	0.000028033	0.000258323	0.28	0.000258323
5	0.000007361	0.000036590	0.000346072	0.46	0.000346072
6	0.000011059	0.000046582	0.000453872	0.73	0.000453872
7	0.000016434	0.000058667	0.000591346	1.13	0.000591346
8	0.000024255	0.000074310	0.000776101	1.74	0.000776101
9	0.000035803	0.000096067	0.001038350	2.64	0.001038349
10	0.000052922	0.000127285	0.001418949	4.00	0.001418948
11	0.000078415	0.000172244	0.001973693	6.05	0.001973690
12	0.000116506	0.000244217	0.002840339	9.11	0.002840331
13	0.000176628	0.000505338	0.005369811	13.71	0.005369759
14	0.000201304	0.000743483	0.007439268	15.38	0.007439130
15	0.000249234	0.001322920	0.012379165	17.89	0.012378533
16	0.000297143	0.002087680	0.018778134	20.40	0.018775927

Table 8: Summary of the results for specimens D1.1/4-1 and B.1/2-1

	Yield moment		Ultimate moment (kN.m)		Displacement (m)	
Test ref.	Aba	Exp	Aba	Exp	Aba	Exp
D1.1/4-1	3.6	3.42	5.10	5.08	0.0202	0.0248
B.1/2-1	14.2	14.60	20.42	20.03	0.0242	0.0232

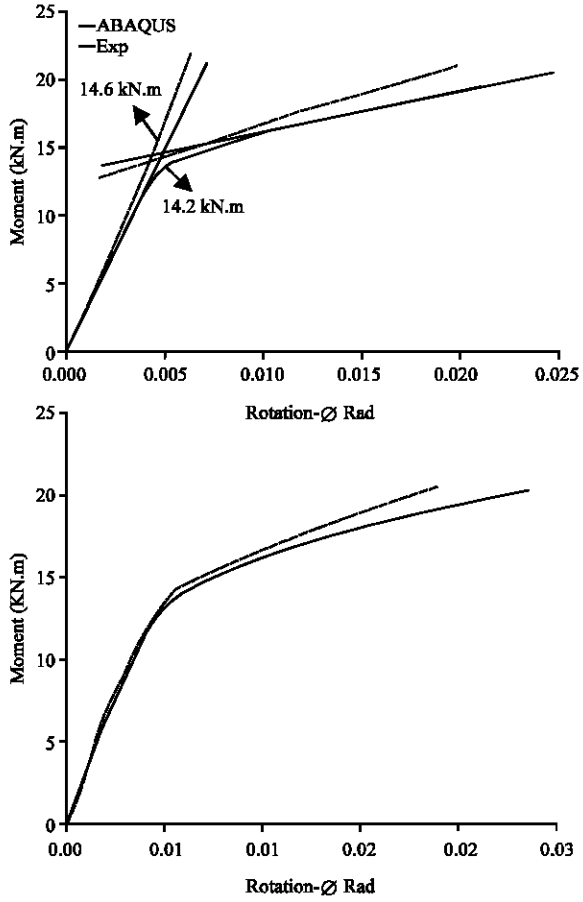

Fig. 18: Moment-rotation (M-Ø) curvefor specimen B.1/2-1

CONCLUSION

The conclusions reported are based on the limited parameters and types of materials used in the present study. The main conclusions are based on the moment-rotation curve and established load-displacement relationships of the 3D non-linear finite element model, it can be seen that linear analysis by using ABAQUS program gives results approximating with experiments and reliable studies. In addition, the results obtained from this study showed convergence and agreement with previous studies that the connection behavior between fully rigid and pinned connection is quite solid and have some rotational stiffness. On the other hand, for all connection studies, the analysis of finite elements using computer software provides a lot of effort and money as compared to a large-scale test and can produce a complete picture of the behavior of joints and deformation, tension and distribution of power and stress.

ACKNOWLEDGEMENT

This research was supported by the Ministry of Higher Education and the University of Malaysia Pahang (UMP) and the researchers would like to thank them for their support.

REFERENCES

Ahmed, A. and R. Hasan, 2015. Effect and evaluation of prying action for top-and seat-angle connections. Intl. J. Adv. Struct. Eng., 7: 159-169.

Azizinamini, A. and J.B. Radziminski, 1989. Static and cyclic performance of semirigid steel beam-to-column connections. J. Struct. Eng., 115: 2979-2999.

Dai, X.H., Y.C. Wang and C.G. Bailey, 2010. Numerical modelling of structural fire behaviour of restrained steel beam-column assemblies using typical joint types. Eng. Struct., 32: 2337-2351.

Danesh, F., A. Pirmoz and A.S. Daryan, 2007. Effect of shear force on the initial stiffness of top and seat angle connections with double web angles. J. Constr. Steel Res., 63: 1208-1218.

Daryan, A.S. and M. Yahyai, 2009. Behavior of bolted top-seat angle connections in fire. J. Constr. Steel Res., 65: 531-541.

Hean, L.S., N.R. Sulong and M. Jameel, 2016. Effect of axial restraints on top-seat angle connections at elevated temperatures. KSCE. J. Civil Eng., 20: 2375-2383.

Kishi, N. and M. Komuro, 2011. Modeling of Connections. In: Semi-Rigid Connections Handbook, Chen, W.F., N. Kishi and M. Komuro (Eds.). J. Ross Publishing, Fort Lauderdale, Florida, ISBN:978-1-932159-99-8, pp: 79-92.

Kukreti, A.R. and A.S. Abolmaali, 1999. Moment-rotation hysteresis behavior of top and seat angle steel frame connections. J. Struct. Eng., 125: 810-820.

Liew, J.R., D.W. White and W.F. Chen, 1993a. Limit states design of semi-rigid frames using advanced analysis: Part 1; Connection modeling and classification. J. Constr. Steel Res., 26: 1-27.

Liew, J.R., D.W. White and W.F. Chen, 1993b. Limit states design of semi-rigid frames using advanced analysis part 2: Analysis and design. J. Constr. Steel Res., 26: 29-57.

Pirmoz, A., A.S. Khoei, E. Mohammadrezapour and A.S. Daryan, 2009. Moment-rotation behavior of bolted top-seat angle connections. J. Constr. Steel Res., 65: 973-984.

Stelmack, T.W., M.J. Marley and K.H. Gerstle, 1986. Analysis and tests of flexibly connected steel frames. J. Struct. Eng., 112: 1573-1588.

Xinwu, W., 2007. Experimental research on hysteretic behavior of top-seat and web angles connections. Proceedings of the 5th WSEAS International Conference on Environment, Ecosystems and Development, December 14-16, 2007, WSEAS, Tenerife, Spain, pp: 75-79.